# Flatness of tracer density profile produced by a point source in turbulence

James P. Gleeson[a)]
*Applied Mathematics, University College Cork, Cork, Ireland*

D. I. Pullin
*Graduate Aeronautical Laboratories, Caltech, Pasadena, California 91125*

(Received 25 November 2002; accepted 18 August 2003; published 1 October 2003)

The average concentration of tracers advected from a point source by a multivariate normal velocity field is shown to deviate from a Gaussian profile. The flatness (kurtosis) is calculated using an asymptotic series expansion valid for velocity fields with short correlation times or weak space dependence. An explicit formula for the excess flatness at first order demonstrates maximum deviation from a Gaussian profile at time $t$ of the order of five times the velocity correlation time, with a $t^{-1}$ decay to the Gaussian value at large times. Monotonically decaying forms of the velocity time correlation function are shown to yield negative values for the first order excess flatness, but positive values can result when the correlation function has an oscillatory tail. © *2003 American Institute of Physics.* [DOI: 10.1063/1.1616558]

## I. INTRODUCTION

The pioneering work of Taylor[1,2] on dispersion problems in turbulent flows has led to the widespread use of Gaussian-plume models for the prediction of mean concentration of passive tracers or pollutants. In isotropic turbulence, for example, the mean tracer concentration may be defined as the probability distribution function (PDF) of particles released from the same point in space, with the statistical ensemble consisting of either independent experiments, or of independent particles released from the source at widely spaced time intervals. This PDF is usually assumed to have a Gaussian form, with variance determined from Taylor's formula.[3] Taylor also argued that the Gaussian form is asymptotically correct for large times, as the particles have effectively executed a random walk through uncorrelated eddies. Moreover, if the turbulent velocity is modeled by a Gaussian (i.e., multivariate normal) velocity field, it immediately follows that the concentration is Gaussian at small times also. Thus it is only at intermediate times that any deviation from a Gaussian distribution might be observed, but few attempts have been made to examine this case.

Kraichnan[4] investigated single-particle diffusion in Gaussian velocity fields using kinematic simulations and the direct-interaction approximation (DIA). His Fig. 9 shows deviations from the Gaussian distribution in numerical experiments, quantified by the flatness factor or kurtosis, which dips below its Gaussian value at intermediate times. Direct-interaction approximations of the flatness were not attempted in Ref. 4, but Koch and Shaqfeh[5] report that DIA calculations lead to an incorrect small-time limit for the flatness in a Gaussian velocity field.

Sawford and Borgas[6] investigated a variety of stochastic models for the Lagrangian velocity in turbulent flow, and showed that a multifractal model[7] and a Markovian jump model (with discontinuous velocities) both predict leptokurtic density functions, i.e., with flatness factors larger than the Gaussian value, although they note the magnitude of the deviation from the Gaussian form depends on the model chosen. Data from wind tunnel experiments is better fitted by a Gaussian distribution than by a leptokurtic distribution, although the difference is not large.

In this paper we utilize an asymptotic series expansion of the mean concentration to derive quadrature formulas for the flatness, and show that simple forms of the velocity time correlation predict a platykurtic (sub-Gaussian flatness) distribution, in agreement with Kraichnan's numerical simulations, but contrary to the models discussed by Sawford and Borgas. The small parameter of our asymptotic series is

$$\alpha = u\tau k_0, \tag{1}$$

where $u$ is the root mean square velocity, $\tau$ is the velocity correlation time, and $k_0$ is a characteristic wavenumber of the energy spectrum [see Eqs. (13) and (14) for full definitions]. We first demonstrate that the concentration is exactly Gaussian in the limit of vanishing $\alpha$: This limit corresponds to either a white-noise in time velocity field ($\tau \to 0$),[3] or to a space-independent velocity ($k_0 \to 0$). We then calculate the flatness using the first few terms in an asymptotic series for small $\alpha$ (Sec. III), and examine some simple examples in Sec. IV. Simplified formulas for terms in the asymptotic series are listed in Appendix A, and in Appendix B Padé approximants are used to show that our results are not restricted to infinitesimally small values of $\alpha$.

## II. EXACT RESULTS

The advection of a tracer from a point source at the origin by a random velocity field is described by the solution of the advection equation

$$\frac{\partial}{\partial t}\theta + \nabla \cdot (\mathbf{u}\theta) = 0, \quad \theta(\mathbf{x},0) = \delta(\mathbf{x}). \tag{2}$$

[a)]Telephone: +353 21 490 3410; fax: +353 21 427 0813. Electronic mail: j.gleeson@ucc.ie

 

Here $\theta d\mathbf{x}$ is the probability, for one realization of the random velocity $\mathbf{u}$ that a marked particle which was at the origin at time $t=0$ will be in the volume element $d\mathbf{x}$ at time $t$. Taking the average over the velocity statistics yields the mean probability density function (or "concentration")

$$\Theta = \langle \theta(\mathbf{x},t) \rangle. \tag{3}$$

In isotropic turbulence the PDF $\Theta$ is a function only of time and the distance $r$ from the source, and so $\Theta(r,t)dr$ is the probability of finding a tracer which was released at the origin at time $t=0$ in the spherical ($d=3$) or circular ($d=2$) shell with radius between $r$ and $r+dr$.

In the following, the velocity will be assumed to be isotropic, with Gaussian (multivariate normal) statistics and mean zero. The effects of molecular diffusion are ignored for clarity, so tracer particles follow the fluid exactly. It is well known that the concentration profile spreads in an approximate Gaussian shape—in particular the width of the cloud is often measured by the dispersion [in this paper we use the isotropic dispersion as defined in (4), which is three times the one-dimensional dispersion used in Ref. 8]

$$D(t) = \langle r^2 \rangle = \int x_\alpha x_\alpha \Theta(\mathbf{x},t) d\mathbf{x}, \tag{4}$$

with the integral being over all of space, and repeated indices summed from 1 to $d$, the number of space dimensions ($d=2$ or 3). Taking $r$ as the distance from the origin, we have $r^2 = x_\alpha x_\alpha$, so $r^2 = x^2 + y^2$ in two dimensions, and $r^2 = x^2 + y^2 + z^2$ in for $d=3$. In a previous paper[8] we addressed the calculation of the dispersion by means of an asymptotic series for small velocity correlation times and confirmed the theoretical results by calculating $\langle r^2 \rangle$ in numerical simulations. It has been noted, however, that the average concentration does not have an exact Gaussian shape for all times.[1,5] The deviation from a Gaussian shape may be measured by the flatness or kurtosis, defined as

$$f(t) = \frac{\langle r^4 \rangle}{\langle r^2 \rangle^2},$$

with $\langle r^4 \rangle$ defined similarly to (4)

$$\langle r^4 \rangle = \int x_\alpha x_\alpha x_\beta x_\beta \Theta(\mathbf{x},t) d\mathbf{x}. \tag{5}$$

The flatness of the distribution $\Theta(\mathbf{x},t)$ is defined as

$$f(t) = \frac{\langle r^4 \rangle}{\langle r^2 \rangle^2} = \frac{\int x_\alpha x_\alpha x_\beta x_\beta \Theta(\mathbf{x},t) d\mathbf{x}}{(\int x_\alpha x_\alpha \Theta(\mathbf{x},t) d\mathbf{x})^2}. \tag{6}$$

The flatness of a $d$-space-dimensional Gaussian distribution is $(2+d)/d$ for all times, as may be confirmed by calculating the integrals in (6) for the general isotropic distribution with zero mean and variance $\sigma^2(t)$:

$$\Theta(\mathbf{x},t) = \frac{1}{(2\pi\sigma^2(t))^{d/2}} \exp\left( -\frac{x_\alpha x_\alpha}{2\sigma^2(t)} \right), \tag{7}$$

to obtain $\langle r^2 \rangle = d\sigma^2$ and $\langle r^4 \rangle = d(2+d)\sigma^4$. Note that for a one-dimensional Gaussian distribution the corresponding flatness $\langle y^4 \rangle / \langle y^2 \rangle^2$ equals 3: It can readily be demonstrated for an isotropic distribution in $d$ space dimensions that $\langle r^2 \rangle = d\langle y^2 \rangle$ and $\langle r^4 \rangle = d\langle y^4 \rangle + d(d-1)\langle y^2 \rangle^2$. Thus the isotropic flatness and the one-dimensional flatness are related by the equation

$$\frac{\langle r^4 \rangle}{\langle r^2 \rangle^2} = \frac{1}{d} \frac{\langle y^4 \rangle}{\langle y^2 \rangle^2} + \frac{d-1}{d}. \tag{8}$$

All our results are expressed in terms of the isotropic flatness.

As an example of an exactly Gaussian concentration profile, consider Eq. (2) when the velocity field is independent of space. The velocity statistics are then fully specified by the covariance

$$\langle u_\alpha(t) u_\beta(t') \rangle = \frac{1}{d} u^2 \delta_{\alpha\beta} R(t-t').$$

We call $R(t)$ the time correlation function of the velocity; note it is symmetric about $t=0$, with $R(0)=1$. In this rather unusual example $R$ must be independent of spatial arguments since the velocity depends only on time; note that in general $R$ is defined through Eq. (12) below. The time correlation is usually assumed to decay to zero as $t$ increases, with a characteristic decay time $\tau$ called the correlation time. The solution for the average concentration can then be shown to be precisely (7) with variance given by

$$\sigma^2(t) = 2u^2 \int_0^t \int_0^{t_1} R(t_1 - t_2) dt_1 dt_2. \tag{9}$$

As (7) is an exact Gaussian form, its flatness is $(2+d)/d$ for all time. In the following we examine how weak space dependence in the velocity field results in a concentration distribution with flatness less than $(2+d)/d$, with maximum deviation near $t=5\tau$. This non-Gaussian flatness is not present in the limit of vanishing correlation time $\tau \to 0$, and so is not seen in models with white-noise in time velocity fields.[3]

## III. ASYMPTOTIC SERIES EXPANSION

### A. Series expansion

We begin by Fourier-transforming all space-dependent variables such as

$$\theta(\mathbf{k},t) = \int \theta(\mathbf{x},t) e^{-i\mathbf{k}\cdot\mathbf{x}} d\mathbf{x}. \tag{10}$$

Henceforth only such Fourier-transformed variables are employed, so the same symbol is used as in physical space. For an isotropic, stationary, and incompressible velocity field in $d$ space dimensions, the covariance is given by

$$\langle u_\alpha(\mathbf{k},t) u_\beta(\mathbf{p},t') \rangle = \delta(\mathbf{k}+\mathbf{p}) Q_{\alpha\beta}(\mathbf{k}, t-t'), \tag{11}$$

with

$$Q_{\alpha\beta}(\mathbf{k},t) = \frac{E(k)R(t,k)}{2(d-1)\pi k^{d-1}} \left( \delta_{\alpha\beta} - \frac{k_\alpha k_\beta}{k^2} \right). \tag{12}$$

Here $E(k)$ is the usual energy spectrum and $R(t,k)$ is the time correlation function of the velocity. The velocity correlation time $\tau$ may be defined by

$$\tau = \int_0^\infty R(t,k)\,dt, \tag{13}$$

and $k_0$ is chosen to be the wavenumber where the spectrum $E(k)$ has its peak. The r.m.s. velocity $u$ is defined by

$$u^2 = \frac{d-1}{d}\int_0^\infty E(k)\,dk. \tag{14}$$

We seek to solve Eq. (2) when the parameter $\alpha$ [defined in terms of $\tau$, $k_0$ and $u$ by Eq. (1)] is significantly smaller than unity.

Equation (2) is transformed to

$$\begin{aligned} &\frac{\partial}{\partial t}\theta(\mathbf{k},t) + i\int d\mathbf{p}\mathbf{k}\cdot\mathbf{u}(\mathbf{p},t)\,\theta(\mathbf{k}-\mathbf{p},t) = 0, \\ &\theta(\mathbf{k},0) = 1, \end{aligned} \tag{15}$$

which may be recast as an integral equation

$$\theta(\mathbf{k},t) = 1 - i\int_0^t dt_1 \int d\mathbf{p}\mathbf{k}\cdot\mathbf{u}(\mathbf{p},t_1)\,\theta(\mathbf{k}-\mathbf{p},t_1). \tag{16}$$

We seek a formal solution of (16) by iteration

$$\begin{aligned} \theta^{(0)} &= 1, \\ \theta^{(1)} &= 1 - i\int_0^t dt_1 \int d\mathbf{p}\mathbf{k}\cdot\mathbf{u}(\mathbf{p},t_1)\,\theta^{(0)}(\mathbf{k}-\mathbf{p},t_1) \\ &= 1 - i\int_0^t dt_1 \int d\mathbf{p}\mathbf{k}\cdot\mathbf{u}(\mathbf{p},t_1), \\ \theta^{(2)} &= 1 - i\int_0^t dt_1 \int d\mathbf{p}\mathbf{k}\cdot\mathbf{u}(\mathbf{p},t_1)\,\theta^{(1)}(\mathbf{k}-\mathbf{p},t_1) \\ &= 1 - i\int_0^t dt_1 \int d\mathbf{p}\mathbf{k}\cdot\mathbf{u}(\mathbf{p},t_1) - \int_0^t dt_1 \int_0^{t_1} dt_2 \\ &\quad \times \int d\mathbf{p} \int d\mathbf{q}\mathbf{k}\cdot\mathbf{u}(\mathbf{p},t_1)(\mathbf{k}-\mathbf{p})\cdot\mathbf{u}(\mathbf{q},t_2). \\ &\quad \vdots \end{aligned} \tag{17}$$

We thus formally construct an infinite series solution to Eq. (15), involving multiple integrals over wavevectors and time. The usefulness of this approach lies in the fact that each term in the infinite series is stochastic only through the appearance of multiple velocity terms, and so the series may be averaged term-by-term to yield a series expansion for $\Theta = \langle\theta\rangle$ of the form

$$\Theta(\mathbf{k},t) = q_0 + \alpha q_1 + \alpha^2 q_2 + \alpha^3 q_3 + \cdots, \tag{18}$$

where $\alpha$ is a bookkeeping parameter whose power equals the number of velocity terms in the corresponding integral, $q_n$ represents the multiple wavevector and time integrals whose integrands depend on the velocity field, and $q_0 = 1$. For a Gaussian velocity field, all even moments may be expressed in terms of the covariance (11), and all odd moments are zero:

$$q_1 = q_3 = q_5 = \cdots = 0.$$

Thus $q_2$, for instance, is given by

$$\begin{aligned} q_2 &= -\int_0^t dt_1 \int_0^{t_1} dt_2 \int d\mathbf{p} \int d\mathbf{q}\langle \mathbf{k}\cdot\mathbf{u}(\mathbf{p},t_1)(\mathbf{k}-\mathbf{p})\cdot\mathbf{u}(\mathbf{q},t_2)\rangle \\ &= -\int_0^t dt_1 \int_0^{t_1} dt_2 \int d\mathbf{p}\mathbf{k}\cdot\mathbf{Q}(\mathbf{p},t_1-t_2)\cdot(\mathbf{k}-\mathbf{p}) \\ &= -\int_0^t dt_1 \int_0^{t_1} dt_2 \int d\mathbf{p}\mathbf{k}\cdot\mathbf{Q}(\mathbf{p},t_1-t_2)\cdot\mathbf{k}, \end{aligned} \tag{19}$$

where we have used (11) and the incompressibility of the velocity field. Contributions to $q_4$ come from the average of four velocity terms, which factors to yield

$$\begin{aligned} q_4 = &\int_0^t dt_1 \int_0^{t_1} dt_2 \int_0^{t_2} dt_3 \int_0^{t_3} dt_4 \int d\mathbf{p} \int d\mathbf{q}[\mathbf{k}\cdot\mathbf{Q}(\mathbf{p},t_1-t_2)\cdot\mathbf{k}][\mathbf{k}\cdot\mathbf{Q}(\mathbf{q},t_3-t_4)\cdot\mathbf{k}] \\ &+ \int_0^t dt_1 \int_0^{t_1} dt_2 \int_0^{t_2} dt_3 \int_0^{t_3} dt_4 \int d\mathbf{p} \int d\mathbf{q}[\mathbf{k}\cdot\mathbf{Q}(\mathbf{p},t_1-t_3)\cdot(\mathbf{k}-\mathbf{q})][(\mathbf{k}-\mathbf{p})\cdot\mathbf{Q}(\mathbf{q},t_2-t_4)\cdot\mathbf{k}] \\ &+ \int_0^t dt_1 \int_0^{t_1} dt_2 \int_0^{t_2} dt_3 \int_0^{t_3} dt_4 \int d\mathbf{p} \int d\mathbf{q}[\mathbf{k}\cdot\mathbf{Q}(\mathbf{p},t_1-t_4)\cdot\mathbf{k}][(\mathbf{k}-\mathbf{p})\cdot\mathbf{Q}(\mathbf{q},t_2-t_3)\cdot(\mathbf{k}-\mathbf{p})]. \end{aligned} \tag{20}$$

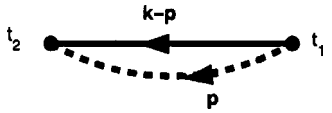


FIG. 1. Diagram of order 1.

The factorization of averages of the Gaussian field into products of velocity covariances leads to a sum of $(2n)!/2^n n!$ terms contributing to $q_{2n}$.

We remark here that the various terms may be accounted for using a diagram expansion method, such as is commonly employed in perturbation expansions over Gaussian fields.[9] First, define the diagrams of order $n$ to be $2n$-polygons with dotted lines joining pairs of vertices. For example, the diagram of order 1 representing Eq. (19) is shown in Fig. 1, with the three diagrams of order 2 (representing $q_4$) in Fig. 2. The expressions for the $q_{2n}$ may be recovered from the diagrams of order $n$ by applying the following diagram rules. Consider the middle diagram of Fig. 2, which represents the second term on the right hand side of (20):

$$\int_0^t dt_1 \int_0^{t_1} dt_2 \int_0^{t_2} dt_3 \int_0^{t_3} dt_4 \int d\mathbf{p} \int d\mathbf{q} [(\mathbf{k}-\mathbf{p})\cdot\mathbf{Q}(\mathbf{p},t_1-t_3) \cdot(\mathbf{k}-\mathbf{q})][(\mathbf{k}-\mathbf{p}-\mathbf{q})\cdot\mathbf{Q}(\mathbf{q},t_2-t_4)\cdot\mathbf{k}]. \tag{21}$$

Observe that (21) may be deduced from the diagram by applying the following rules:

(1) Vertex labels are the time integration variables.

(2) The wavevector integration variables are the wavevectors labeling the internal dotted lines; these integrals are over all wavevector space.

(3) The vector sum of wavevectors at each vertex is zero, except for the first vertex (labeled $t_1$) which has sum $+\mathbf{k}$, and the final vertex which has sum $-\mathbf{k}$.

To compose the integrand, we multiply the factors resulting from each of the following rules:

(4) For each internal dotted line, consider the start and end vertices. In the diagram example above, for the internal dotted line labeled $\mathbf{p}$, the start vertex is labeled $t_1$ and the end vertex is labeled $t_3$. Both the start and the end vertex have solid lines emanating from them; suppose the wavevector labels on these lines are $\mathbf{a}$ and $\mathbf{b}$, respectively. Then the factor we seek is $-\mathbf{a}\cdot\mathbf{Q}(\mathbf{p},t_s-t_e)\cdot\mathbf{b}$ where $\mathbf{p}$ is the dotted line label and $t_s$ and $t_e$ are the start and end vertex labels. (If the end vertex is the last vertex, then let $\mathbf{b}=\mathbf{k}$.) In the example, $\mathbf{a}=\mathbf{k}-\mathbf{p}$ and $\mathbf{b}=\mathbf{k}-\mathbf{q}$, so that the factor is $-(\mathbf{k}-\mathbf{p})\cdot\mathbf{Q}(\mathbf{p},t_1-t_3)\cdot(\mathbf{k}-\mathbf{q})$. By applying this rule again to the second dotted line, we find another factor of $-(\mathbf{k}-\mathbf{p}-\mathbf{q})\cdot\mathbf{Q}(\mathbf{q},t_2-t_4)\cdot\mathbf{k}$. Further simplification may be possible due to incompressibility.

These rules form an algorithm for finding the $q_{2n}$ terms in the iteration expansion of $\Theta$ and so may be implemented using a symbolic manipulation program like MATHEMATICA.

### B. Renormalization

The behavior of each diagram as time increases determines the quality of the approximation to $\Theta$ resulting from truncating the infinite series. If the time correlation function $R(t,k)$ decays sufficiently quickly (e.g., exponentially) to zero as $t\to\infty$, it can be shown that *connected* diagrams, i.e., those which cannot be split into two separate parts by cutting one solid line, grow linearly in time and so their contribution to $\partial\Theta/\partial t$ remains bounded as $t\to\infty$. On the other hand, *unconnected diagrams* such as the first term on the right hand side of (20) grow faster than linearly, and their contribution to $\partial\Theta/\partial t$ is unbounded. With a view to renormalizing the infinite series (18) to eliminate these secular effects, we consider simple equivalent equations describing the evolution of the PDF $\Theta$. For example, the functional-derivative closure (FDC) method advanced in Ref. 8 leads to an integrodifferential equation for $\Theta$

$$\frac{\partial\Theta}{\partial t} = \int_0^t K_1(\mathbf{k},s)\Theta(\mathbf{k},s)ds, \tag{22}$$

and an asymptotic expansion is derived for the kernel $K_1$. However, following the method of cumulant expansion,[9,10] we suggest that a simpler ansatz

$$\frac{\partial\Theta}{\partial t} = K(\mathbf{k},t)\Theta(\mathbf{k},t), \tag{23}$$

is equally as effective a renormalization, and indeed generates the same results as the FDC method with a significant reduction in the complexity of algebraic manipulations. Noting that the solution to (23) satisfying the initial condition is

$$\Theta(\mathbf{k},t) = \exp\left[\int_0^t K(\mathbf{k},T)dT\right], \tag{24}$$

it remains only to find an expression for $K$ as a cumulant expansion.

We seek an expansion for $K$ in even powers of $\alpha$

$$K = K_0 + \alpha^2 K_2 + \alpha^4 K_4 + \cdots, \tag{25}$$

and utilize this and (18) into (23) to match coefficients of powers of $\alpha$ term-by-term

$$\alpha^2\frac{\partial q_2}{\partial t} + \alpha^4\frac{\partial q_4}{\partial t} + \cdots = (K_0 + \alpha^2 K_2 + \alpha^4 K_4 + \cdots) \times (q_0 + \alpha^2 q_2 + \alpha^4 q_4 + \cdots), \tag{26}$$

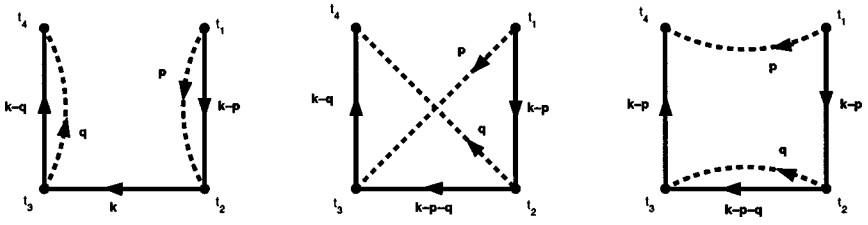


FIG. 2. The three diagrams of order 2.

yielding the $K_n$ in terms of the known $q_n$

$$K_0=0, \quad K_2=\frac{1}{q_0}\frac{\partial q_2}{\partial t},$$
$$K_4=\frac{1}{q_0}\left[\frac{\partial q_4}{\partial t}-\frac{q_2}{q_0}\frac{\partial q_2}{\partial t}\right]. \tag{27}$$
$$\vdots$$

Thus, for example, $K_2$ is found from (19) to be

$$K_2=-\int_0^t dt_2 \int d\mathbf{p}\mathbf{k}\cdot\mathbf{Q}(\mathbf{p},t-t_2)\cdot\mathbf{k}, \tag{28}$$

and again, each $K_n$ may be calculated using symbolic manipulation computer packages. Moreover, it is found that the undesirable growth of terms as $t\to\infty$ noted above is not present in the expansion for $K$, thus allowing us to use (24) as an approximation to $\Theta$ over all time.

### C. Flatness of the Θ PDF

Having found an expansion for the probability density function of tracers (24), it remains only to use this to calculate the flatness of the distribution, according to Eq. (6). In terms of the Fourier transformed variables, the moments such as (5) may be written as

$$\langle r^4\rangle=\frac{\partial^4}{\partial k_\alpha \partial k_\alpha \partial k_\beta \partial k_\beta}\Theta(\mathbf{k},t)\big|_{\mathbf{k}=\mathbf{0}}, \tag{29}$$

and for an isotropic distribution (i.e., $\Theta$ depending only on magnitude $k$ of $\mathbf{k}$, independent of orientation) in $d$ dimensions this reduces to

$$\langle r^4\rangle=\frac{d(2+d)}{3}\frac{\partial^4}{\partial k^4}\Theta(k,t)\big|_{k=0}. \tag{30}$$

Similarly, the isotropic second moment is

$$\langle r^2\rangle=-d\frac{\partial^2}{\partial k^2}\Theta(k,t)\big|_{k=0},$$

and so the flatness (6) is

$$f(t)=\frac{2+d}{3d}\frac{\left.\frac{\partial^4\Theta}{\partial k^4}\right|_{k=0}}{\left(-\left.\frac{\partial^2\Theta}{\partial k^2}\right|_{k=0}\right)^2}, \tag{31}$$

which is written in terms of $K$ using (24)

$$f(t)=\frac{2+d}{3d}\left[3+\frac{\frac{\partial^4}{\partial k^4}\int_0^t K(k,T)dT\big|_{k=0}}{\left(-\frac{\partial^2}{\partial k^2}\int_0^t K(k,T)dT\Big|_{k=0}\right)^2}\right]. \tag{32}$$

Using the expansion (25) of $K$ derived above, it is straightforward to calculate the derivatives in (32) term-by-term; for convenience we introduce the notation

$$D_n=-\frac{\partial^2}{\partial k^2}\int_0^t K_n(k,T)dT\big|_{k=0},$$
$$F_n=\frac{\partial^4}{\partial k^4}\int_0^t K_n(k,T)dT\big|_{k=0}, \tag{33}$$

and so (32) becomes

$$f(t)=\frac{2+d}{3d}\left[3+\frac{\Sigma_{n=1}^{\infty}\alpha^{2n}F_{2n}(t)}{(\Sigma_{n=1}^{\infty}\alpha^{2n}D_{2n}(t))^2}\right]. \tag{34}$$

Noting that $F_2=F_4=0$, we list in Appendix A the formulas for $F_6$ and $D_2$ to $D_6$, having performed all angular integrals, and so reducing the expressions to multiple integrals over time and wavenumbers.

## IV. TIME CORRELATION FUNCTIONS

The calculation of the tracer flatness for a given perturbation parameter $\alpha$ has been reduced to the evaluation of the quantities $D_n$ and $F_n$ as in Eq. (34). In this section some simple time correlation functions are chosen to demonstrate the lowest-order perturbation results. Padé approximants are employed in Appendix B to support the claim that the results presented here are qualitatively correct for noninfinitesimal $\alpha$.

### A. Exponential time correlation

To simplify the analysis we take the time correlation function to have the following form:

$$R(t,k)=e^{-\omega|t|}, \tag{35}$$

where $\omega=\tau^{-1}$ is the inverse of the velocity correlation time. This is a rather unrealistic approximation to the time correlation of turbulent velocity fields, chiefly because it is not differentiable at $t=0$, and also due to its lack of dependence on the wavenumber $k$ (see Refs. 8 and 11). However, it results in a number of simplifications of our analysis which enable the structure of the expansion to be clearly shown; we note further that numerical computation by quadrature is always possible in the general case. Such a quadrature computation is performed for a correlation function which is smooth at $t=0$ in the next section, and the flatness behaves similarly to the analytical results derived here.

With $R$ independent of wavenumber, the integrals over $p$, $q$, and $r$ reduce to moments of the energy spectrum, for which we introduce the notation

$$m_i=\frac{d-1}{d}\int_0^\infty k^i E(k)dk. \tag{36}$$

The factor of $(d-1)/d$ ensures the simple identification $m_0=u^2$. Note that if $R$ is wavenumber-dependent, then the full quadrature expressions given in Appendix A must be evaluated, whereas assuming $R$ to depend only on the time difference allows us to evaluate all wavenumber integrals in terms of the moments (36) of the energy spectrum.

We now nondimensionalize variables by a characteristic wavenumber $k_0$ and the correlation time $\omega^{-1}$, and note that the bookkeeping parameter emerges naturally as the nondimensional number

$$\alpha = \frac{uk_0}{\omega}. \tag{37}$$

Further simplification follows by using (35) and introducing the Laplace transform

$$\tilde{D}(s) = \int_0^\infty e^{-st} D(t)\,dt,$$

so that the series expansion of the dispersion $D(t)$ transforms to

$$\tilde{D}(s) = \alpha^2 \tilde{D}_2(s) + \alpha^4 \tilde{D}_4(s) + \cdots, \tag{38}$$

with

$$\tilde{D}_2(s) = 2u^2 \frac{1}{s^2(s+1)} \tag{39}$$

and

$$\tilde{D}_4(s) = -2u^2 m_2 \frac{1}{s^2(s+1)^2(s+2)}. \tag{40}$$

Similarly, the Laplace transform of the fourth tracer moment is

$$\tilde{F}(s) = \alpha^2 \tilde{F}_2(s) + \alpha^4 \tilde{F}_4(s) + \alpha^6 \tilde{F}_6(s) + \cdots, \tag{41}$$

with

$$\tilde{F}_2(s) = \tilde{F}_4(s) = 0, \tag{42}$$

and, for $d=3$,

$$\tilde{F}_6^{3D}(s) = -\frac{144u^4 m_2 (5s+8)}{5s^2(s+1)^3(s+2)^2(s+3)}. \tag{43}$$

The two-dimensional versions of $D$ have the same form as above, but the $F_6$ term must be multiplied by 5/4 to go from the three-dimensional (43) to the two-dimensional equivalent:

$$\tilde{F}_6^{2D}(s) = -\frac{36u^4 m_2 (5s+8)}{s^2(s+1)^3(s+2)^2(s+3)}. \tag{44}$$

Each of the series may be viewed as asymptotic expansions about $\alpha=0$, as they are clearly power series in even powers of $\alpha$. Recalling the definition of $\alpha$ as $uk_0/\omega$, we identify the $\alpha\to 0$ limit as the limit of small correlation time (white noise in time, $\omega\to\infty$), or of a weak space dependence of the velocity field ($k_0\to 0$). The latter interpretation is related to the exact solution discussed in Sec. II. We showed there that a velocity field that depends only on time leads to a tracer concentration which is exactly Gaussian. Being independent of space means that the energy spectrum is a delta function: $E(k)\propto\delta(k)$, so all moments $m_n$ are zero and all terms in the series for $F$ vanish identically.

The limiting behavior of $D_n(t)$ and $F_n(t)$ as $t\to 0$ may be found by inverting the Laplace transform, or more simply by expanding the transforms $\tilde{D}_n(s)$ and $\tilde{F}_n(s)$ about $s=\infty$, then reading off the coefficient of $t^n$ as $1/n!$ times the coefficient of $s^{-(n+1)}$. We find

$$D_2(t) = u^2 t^2 + O(t^3), \tag{45}$$

$$D_4(t) = -\tfrac{1}{12} u^4 m_2 t^4 + O(t^5), \tag{46}$$

$$F_6^{3D}(t) = -\tfrac{1}{5} u^4 m_2 t^6 + O(t^7), \tag{47}$$

$$F_6^{2D}(t) = -\tfrac{1}{4} u^4 m_2 t^6 + O(t^7) \quad \text{as} \quad t\to 0, \tag{48}$$

and in general

$$D_{2n}(t) = O(t^{2n}), \quad F_{2n}(t) = O(t^{2n}) \quad \text{as} \quad t\to 0. \tag{49}$$

Similarly the limit as $t\to\infty$ may be found without inverting the Laplace transform by expanding it into partial fractions of the form

$$\frac{A_1}{s^2} + \frac{A_2}{s} + \sum_{i=1}^{l} \frac{B_i}{(s-b_i)^{n_i}} + \cdots, \tag{50}$$

which inverts to

$$A_1 t + A_2 + \text{exponentially decaying terms},$$

provided that the poles $b_i$ all have negative real part. Using this, we find

$$D_2(t) = 2u^2 t + o(t), \tag{51}$$

$$D_4(t) = -u^2 m_2 t + o(t), \tag{52}$$

$$F_6^{3D}(t) = -\tfrac{96}{5} u^4 m_2 t + o(t), \tag{53}$$

$$F_6^{2D}(t) = -24u^4 m_2 t + o(t) \quad \text{as} \quad t\to\infty, \tag{54}$$

with the general result being

$$D_n(t) = O(t), \quad F_n(t) = O(t) \quad \text{as} \quad t\to\infty. \tag{55}$$

Consider the flatness when $\alpha \ll 1$, i.e., when the correlation time is short or the velocity is only weakly space-dependent. Then we approximate $F$ and $D$ by the first nonzero terms in their expansions

$$D(t) \approx \alpha^2 D_2(t), \quad F(t) \approx \alpha^6 F_6(t),$$

and find the flatness from (34) to be

$$f(t) \approx \frac{2+d}{3d}\left[3 + \alpha^2 \frac{F_6(t)}{(D_2(t))^2}\right].$$

As the limit $\alpha\to 0$ corresponds to the exactly Gaussian case, we define the *excess flatness* as

$$f_\alpha(t) = \frac{1}{m_2}\frac{F_6(t)}{(D_2(t))^2}. \tag{56}$$

From the limits discussed above, it is clear that the excess flatness approaches zero as $t\to 0$ and as $t\to\infty$. Inverting (39) and (43) yields an analytical expression for the excess flatness:

$$f_\alpha^{3D}(t)=\frac{-2(24t-89)-7e^{-3t}-18(2t+1)e^{-2t}-9(6t^2+14t+17)e^{-t}}{10(t-1+e^{-t})^2}. \tag{57}$$

The corresponding two-dimensional value is obtained by multiplying (57) by 5/4. The minimum near $t=5$ (see Fig. 3) is accurately determined numerically to demonstrate that the maximum deviation from the Gaussian flatness occurs at (dimensional) time

$$t=5.0630\omega^{-1}, \tag{58}$$

with flatness

$$f^{3D}=\tfrac{5}{9}[3+\alpha^2 m_2 f_\alpha^{3D}(5.0630)]=\tfrac{5}{3}-0.264\,346\alpha^2 m_2. \tag{59}$$

Similarly, the two-dimensional minimum flatness is

$$f^{2D}=2-0.396\,518\alpha^2 m_2. \tag{60}$$

As $t\to\infty$, the excess flatness returns to zero from below; its asymptotic form can be found readily from (57), or using (51) and (53) to be

$$f_\alpha^{3D}(t)\sim-\frac{24}{5}\frac{1}{t}+o\left(\frac{1}{t}\right), \tag{61}$$

$$f_\alpha^{2D}(t)\sim-\frac{6}{t}+o\left(\frac{1}{t}\right)\ \text{ as }\ t\to\infty. \tag{62}$$

In Appendix B a simple energy spectrum is used to calculate higher order terms in the flatness, and Padé approximants extend the conclusions reached here to noninfinitesimal values of $\alpha$.

### B. Other time correlation functions

Equation (35) assumes a monotonically decaying time correlation. It was shown in Ref. 8 that the asymptotic series for the dispersion has different forms depending on whether the time correlation function decays monotonically to zero, or has an oscillatory tail. We therefore consider here a generalization of (35) which has a nonmonotonic decay to zero:

$$R(t,k)=e^{-\omega|t|}\cos(at). \tag{63}$$

The Laplace transform techniques of the previous section are also applicable here, and the excess flatness may again be expressed as (56). However, even with the aid of Laplace transforms, the expression for $F_6$ is algebraically complicated and so the detailed form is omitted here (but may be obtained from the corresponding author). The asymptotic behavior of the excess flatness is given by

$$f_\alpha^{3D}(t)\sim-\frac{24}{5}\frac{1-3a^2}{(1+a^2)^3}\frac{1}{t}+o\left(\frac{1}{t}\right)\ \text{ as }\ t\to\infty, \tag{64}$$

which reduces to (61) at $a=0$. A similar generalization of (62) holds in two dimensions. Note that the excess flatness decays to zero from above if $a>1/\sqrt{3}$. This behavior, and the appearance of oscillations in $f_\alpha(t)$ are shown in Fig. 4.

As a final example of the $O(\alpha^2)$ excess flatness, we consider the time correlation function

$$R(t,k)=e^{-\omega^2 t^2/2}. \tag{65}$$

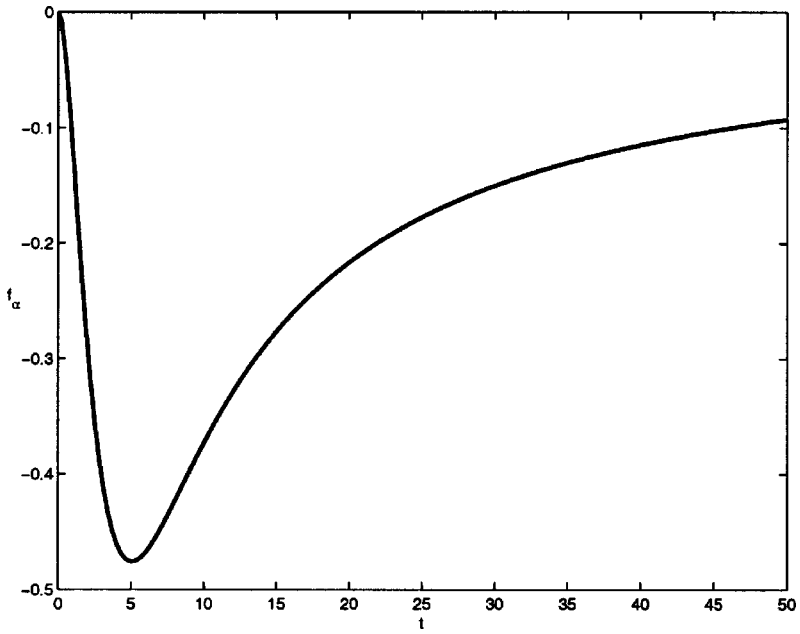


FIG. 3. First order excess flatness (57) for exponential time correlation.

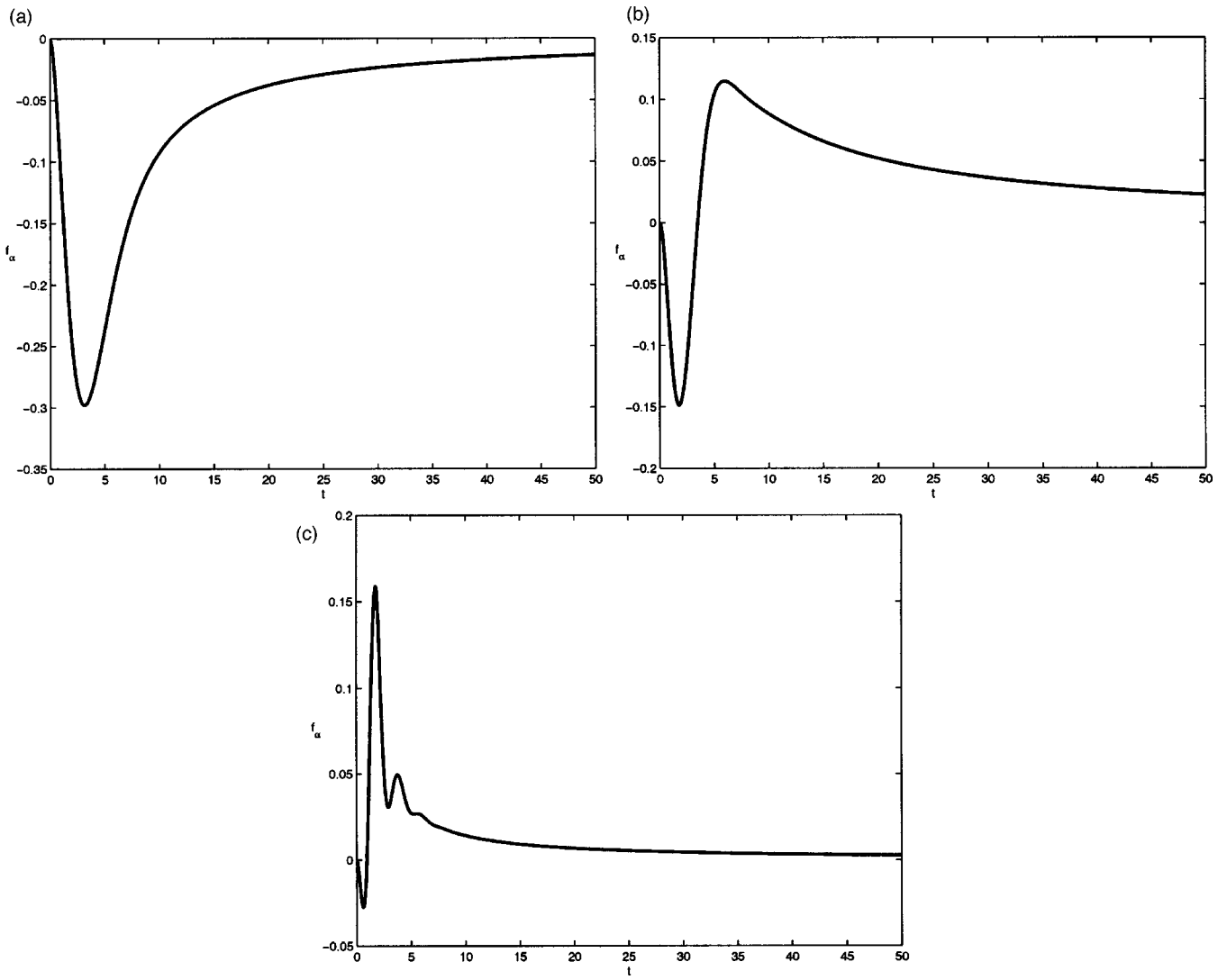


FIG. 4. First order excess flatness for oscillatory time correlation, for various values of $a$: (a) $a=0.5$, (b) $a=1$, (c) $a=3$.

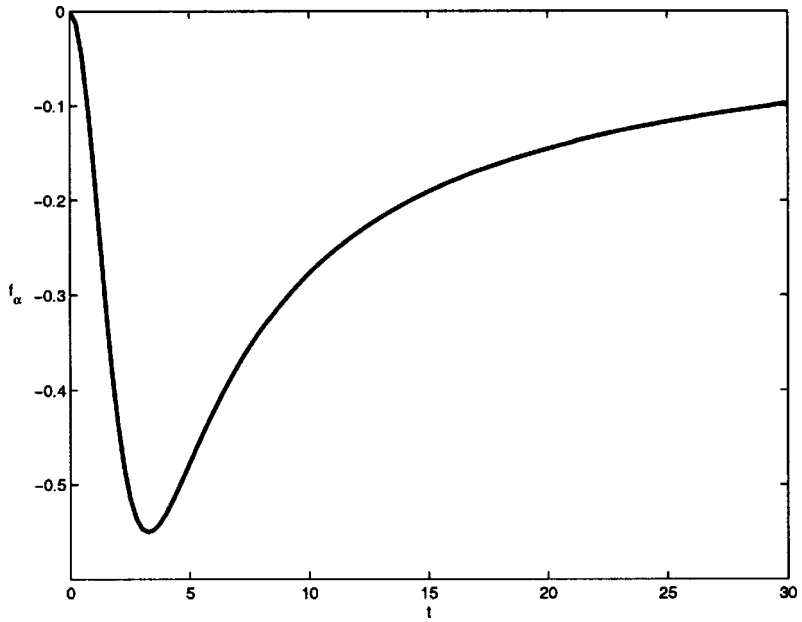


FIG. 5. First order excess flatness in three dimensions for time correlation function (65).

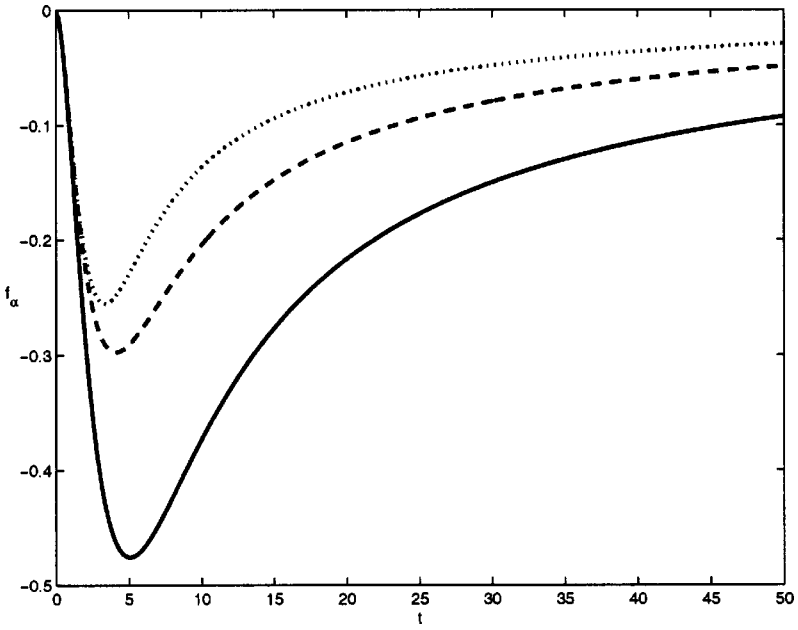


FIG. 6. Padé approximants $f^{[0,0]}$ (solid), $f^{[0,1]}$ (dashed), and $f^{[1,1]}$ (dotted) in three dimensions, with $\alpha=0.75$.

In this case the time integrals must be calculated numerically; see Fig. 5 for the three-dimensional case. Again, the two-dimensional flatness is 5/4 times the three-dimensional value. Note the negative excess near $t=5$ and slow return to zero excess flatness as $t\to\infty$, similar to that found analytically for the exponential time correlation function. We conclude that the properties of the flatness demonstrated in the previous section are not strongly dependent upon the smoothness of $R$ at $t=0$.

## V. CONCLUSION

We have described an asymptotic series expansion for the PDF of tracers (i.e., mean concentration field) advected by a Gaussian random velocity field in the form of a cumulant expansion. As noted following Eq. (23), the renormalization procedure which ensures that the series is nonsecular in time is not unique, but the approach taken here is algebraically simpler than, for instance, the functional-derivative closure method of Ref. 8, and leads to the same results.

Our main result is Eq. (34) for the tracer flatness along with the quadrature expressions for $D_n$ and $F_n$ given in Appendix A. In principle, these imply that the tracer flatness is fully specified once the energy spectrum and the time correlation function $R$ of the velocity field are given. We have examined some particularly interesting examples in Sec. IV, which include an analytic formula (57) for the flatness when $R$ is an exponential function, and a generalization to the case where $R$ has an oscillatory tail. Numerical quadrature for a smooth monotonic $R$ yields similar results to the analytical expression (57), and Padé approximants (Appendix B) extend the result beyond infinitesimal values of $\alpha$, at least for the single-scale energy spectrum (66).

The conclusion to be drawn from Figs. 3, 5, and 6 and the formulas for $F_6$ in Appendix A is that the tracer PDF is platykurtic (i.e., has negative excess flatness) when the velocity correlation function $R$ is monotonically decaying in time, at least for low values of the parameter $\alpha$. This conclusion is supported by Kraichnan's numerical simulations for finite values of $\alpha$,[4] but contradicts the predictions of two models in Ref. 6. Interestingly, the excess flatness can exhibit positive values when $R$ has an oscillatory tail, see Fig. 4. It would be interesting to extend Kraichnan's[4] kinematic simulations to examine such cases; indeed we hope the present work will stimulate such studies. These could be performed by sequentially releasing particles from a single fixed point in space into a velocity field generated as a sum of random Fourier modes.[4] The accurate computation of trajectories for a sufficiently large number of particles should, in principle, allow construction of the moments of the particle radial density distribution, and hence of the flatness. Further work is also required to calculate the flatness when $R$ depends nontrivially on the wavenumber as well as on the time difference.

## ACKNOWLEDGMENTS

This project was partly funded by the Enterprise Ireland International Collaboration Fund, Science Foundation Ireland Investigator Award 02/IN.1/IM062, and by a research grant from the Faculty of Arts, University College Cork.

## APPENDIX A: HIGHER-ORDER TERMS IN EQ. (34)

The asymptotic series expansion detailed in Sec. III leads to expression (33) for the flatness, involving multiple integrals over wavevectors and time. The angular integrals may be performed exactly, and so the reduced forms for the isotropic $D_{2n}$ and $F_{2n}$ for $n\leqslant 3$ in three dimensions are as follows. Note that these expressions include general wavenumber dependence in the time correlation function $R$; further simplification follows when wavenumber-independent correlation functions are considered as in Sec. IV and Appendix B.

$$D_2^{3D}=\frac{4}{3}\int_0^t dt_1\int_0^{t_1} dt_2\int_0^\infty dpE(p)R(t_1-t_2,p),$$

$$D_4^{3D}=-\frac{8}{9}\int_0^t dt_1\int_0^{t_1} dt_2\int_0^{t_2} dt_3\int_0^{t_3} dt_4\int_0^\infty dp\int_0^\infty dqp^2E(p)E(q)R(t_1-t_4,p)R(t_2-t_3,q),$$

$$\begin{aligned}D_6^{3D}=&\int_0^\infty dp\int_0^\infty dq\int_0^\infty dr\int_0^t dt_1\int_0^{t_1} dt_2\int_0^{t_2} dt_3\int_0^{t_3} dt_4\int_0^{t_4} dt_5\int_0^{t_5} dt_6E(p)E(q)E(r)\\&\times\left[\frac{16p^4}{27}R(t_1-t_6,p)R(t_2-t_5,q)R(t_3-t_4,r)+\frac{16p^2q^2}{27}R(t_1-t_6,p)R(t_2-t_5,q)R(t_3-t_4,r)\right.\\&+\frac{16p^4}{27}R(t_1-t_6,p)R(t_2-t_4,q)R(t_3-t_5,r)+\frac{16p^4}{27}R(t_1-t_6,p)R(t_2-t_3,q)R(t_4-t_5,r)\\&-\frac{16p^2q^2}{135}R(t_1-t_5,p)R(t_2-t_6,q)R(t_3-t_4,r)-\frac{8p^2q^2}{135}R(t_1-t_4,p)R(t_2-t_6,q)R(t_3-t_5,r)\\&\left.-\frac{8p^2r^2}{135}R(t_1-t_5,p)R(t_2-t_4,q)R(t_3-t_6,r)-\frac{8p^2r^2}{135}R(t_1-t_4,p)R(t_2-t_5,q)R(t_3-t_6,r)\right],\end{aligned}$$

$$F_2^{3D}=0,$$

$$F_4^{3D}=0,$$

$$\begin{aligned}F_6^{3D}=&-\frac{64}{45}\int_0^\infty dp\int_0^\infty dq\int_0^\infty dr\int_0^t dt_1\int_0^{t_1} dt_2\int_0^{t_2} dt_3\int_0^{t_3} dt_4\int_0^{t_4} dt_5\int_0^{t_5} dt_6E(p)E(q)E(r)\\&\times[4p^2R(t_1-t_6,p)R(t_2-t_5,q)R(t_3-t_4,r)+4p^2R(t_1-t_6,p)R(t_2-t_4,q)R(t_3-t_5,r)\\&+4p^2R(t_1-t_6,p)R(t_2-t_3,q)R(t_4-t_5,r)+(2p^2+2q^2)R(t_1-t_5,p)R(t_2-t_6,q)R(t_3-t_4,r)\\&+(p^2+2q^2)R(t_1-t_4,p)R(t_2-t_6,q)R(t_3-t_5,r)+2q^2R(t_1-t_3,p)R(t_2-t_6,q)R(t_4-t_5,r)\\&+(2p^2+r^2)R(t_1-t_5,p)R(t_2-t_4,q)R(t_3-t_6,r)+(p^2+q^2+r^2)R(t_1-t_4,p)R(t_2-t_5,q)R(t_3-t_6,r)\\&+2p^2R(t_1-t_5,p)R(t_2-t_3,q)R(t_4-t_6,r)+q^2R(t_1-t_3,p)R(t_2-t_5,q)R(t_4-t_6,r)].\end{aligned}$$

In two dimensions, the corresponding expressions are

$$D_2^{2D}=\int_0^t dt_1\int_0^{t_1} dt_2\int_0^\infty dpE(p)R(t_1-t_2,p),$$

$$D_4^{2D}=-\frac{1}{2}\int_0^t dt_1\int_0^{t_1} dt_2\int_0^{t_2} dt_3\int_0^{t_3} dt_4\int_0^\infty dp\int_0^\infty dqp^2E(p)E(q)R(t_1-t_4,p)R(t_2-t_3,q),$$

$$\begin{aligned}D_6^{2D}=&\int_0^\infty dp\int_0^\infty dq\int_0^\infty dr\int_0^t dt_1\int_0^{t_1} dt_2\int_0^{t_2} dt_3\int_0^{t_3} dt_4\int_0^{t_4} dt_5\int_0^{t_5} dt_6E(p)E(q)E(r)\\&\times\left[\frac{p^4}{4}R(t_1-t_6,p)R(t_2-t_5,q)R(t_3-t_4,r)+\frac{p^2q^2}{4}R(t_1-t_6,p)R(t_2-t_5,q)R(t_3-t_4,r)\right.\\&+\frac{p^4}{4}R(t_1-t_6,p)R(t_2-t_4,q)R(t_3-t_5,r)+\frac{p^4}{4}R(t_1-t_6,p)R(t_2-t_3,q)R(t_4-t_5,r)\\&-\frac{p^2q^2}{8}R(t_1-t_5,p)R(t_2-t_6,q)R(t_3-t_4,r)-\frac{p^2q^2}{16}R(t_1-t_4,p)R(t_2-t_6,q)R(t_3-t_5,r)\\&\left.-\frac{p^2r^2}{16}R(t_1-t_5,p)R(t_2-t_4,q)R(t_3-t_6,r)-\frac{p^2r^2}{16}R(t_1-t_4,p)R(t_2-t_5,q)R(t_3-t_6,r)\right],\end{aligned}$$

$$F_2^{2D}=0,\quad F_4^{2D}=0,\quad F_6^{2D}=\frac{135}{256}F_6^{3D}.$$

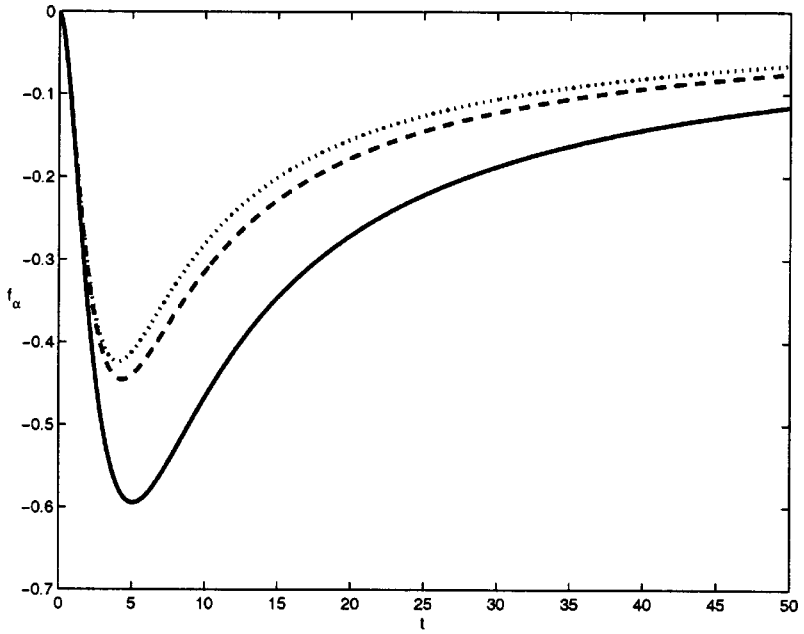


FIG. 7. Padé approximants $f^{[0,0]}$ (solid), $f^{[0,1]}$ (dashed), and $f^{[1,1]}$ (dotted) in two dimensions, with $\alpha=0.5$.

## APPENDIX B: PADÉ APPROXIMANTS

In order to extend the analysis to include higher powers of $\alpha$, it is convenient to adopt the exponential time correlation function (35) and a single-scale (dimensional) energy spectrum

$$E(k)=\frac{d}{d-1}u^2\delta(k-k_0), \tag{66}$$

which allows us to set all moments of the energy spectrum to unity, $m_n=1$ (having nondimensionalized with $k_0$ and $\omega$ as before).

Even with this simplification, the higher order terms involve significant symbolic manipulation, and result in complicated expressions for $\tilde{D}_6$, $\tilde{D}_8$, $\tilde{F}_8$, and $\tilde{F}_{10}$, which are omitted here for brevity. Having calculated these higher order terms in the asymptotic series, we use Padé approximants[12] to accelerate convergence of the asymptotic series. We note that such methods were used successfully in Ref. 8 for the related problem of calculating turbulent diffusivities. Padé approximants to $D$ and $F$ are defined as rational functions of $\alpha$ which yield the correct asymptotic series for small $\alpha$:

$$D^{[0,0]}(t)=D_2(t),\quad D^{[0,1]}(t)=\frac{D_2(t)}{1-\alpha^2\dfrac{D_4(t)}{D_2(t)}},$$

$$D^{[1,1]}(t)=\frac{D_2+\alpha^2\dfrac{D_4^2-D_2D_6}{D_4}}{1-\alpha^2\dfrac{D_6}{D_4}},$$

$$F^{[0,0]}(t)=F_6(t),\quad F^{[0,1]}(t)=\frac{F_6(t)}{1-\alpha^2\dfrac{D_8(t)}{D_6(t)}},$$

$$F^{[1,1]}(t)=\frac{F_6+\alpha^2\dfrac{F_8^2-F_6F_{10}}{F_8}}{1-\alpha^2\dfrac{F_{10}}{F_8}}.$$

The excess flatness is thus successively approximated by

$$f^{[0,0]}=\frac{F^{[0,0]}}{(D^{[0,0]})^2},\quad f^{[0,1]}=\frac{F^{[0,1]}}{(D^{[0,1]})^2},\quad f^{[1,1]}=\frac{F^{[1,1]}}{(D^{[1,1]})^2},$$

and yields curves that lie close together for $\alpha$ on the order of 1/2, see Figs. 6 and 7 for the three- and two-dimensional cases, respectively. The fact that successive Padé approximants lie close together may heuristically be taken to indicate that the exact value of the excess flatness is indeed negative even when $\alpha$ is not infinitesimally small, and so the PDF $\Theta$ is platykurtic (has sub-Gaussian flatness). This is supported by the numerical simulations of Kraichnan,[4] which are performed at relatively high values of $\alpha$, and is contrary to the predictions of the multifractal and Markovian jump models examined by Sawford and Borgas.[6]

[1] G. I. Taylor, "Diffusion by continuous movements," Proc. London Math. Soc. **20**, 196 (1921).
[2] A. S. Monin and A. M. Yaglom, *Statistical Fluid Mechanics: Mechanics of Turbulence* (MIT Press, Cambridge, Massachusetts, 1971).
[3] G. Falkovich, K. Gawedzki, and M. Vergassola, "Particles and fields in fluid turbulence," Rev. Mod. Phys. **73**, 913 (2001).
[4] R. H. Kraichnan, "Diffusion by a random velocity field," Phys. Fluids **13**, 22 (1970).
[5] D. L. Koch and E. S. G. Shaqfeh, "Averaged-equation and diagrammatic approximations to the average concentration of a tracer advected by a Gaussian random velocity field," Phys. Fluids A **4**, 887 (1992).
[6] B. L. Sawford and M. S. Borgas, "On the continuity of stochastic models for the Lagrangian velocity in turbulence," Physica D **76**, 297 (1994).
[7] M. S. Borgas and B. L. Sawford, "Stochastic equations with multifractal random increments for modeling turbulent dispersion," Phys. Fluids **6**, 618 (1994).

[8]J. P. Gleeson, ''A closure method for random advection of a passive scalar,'' Phys. Fluids **12**, 1472 (2000).
[9]A. H. Nayfeh, *Perturbation Methods* (Wiley Interscience, New York, 1973), Sec. 7.4.
[10]N. G. Van Kampen, *Stochastic Processes in Physics and Chemistry* (Elsevier Science, New York, 1992), Sec. XVI.3.
[11]W. D. McComb, V. Shanmugasundaram, and P. Hutchison, ''Velocity-derivative skewness and two-time correlations of isotropic turbulence as predicted by the LET theory,'' J. Fluid Mech. **208**, 91 (1989).
[12]G. A. Baker, *Essentials of Padé Approximants* (Academic, New York, 1975).